# Design and operation of a two-stage positron accumulator

J. Clarke, D. P. van der Werf, B. Griffiths, D. C. S. Beddows, M. Charlton, H. H. Telle, and P. R. Watkeys
*Department of Physics, University of Wales Swansea, Singleton Park, Swansea SA2 8PP, United Kingdom*

(Received 23 January 2006; accepted 6 March 2006; published online 12 June 2006)

A compact positron accumulator based upon a simple two-stage buffer gas cooling scheme is described. Its operation to produce 10–20 ns wide bursts containing around $10^5$ positrons with cycling times in the 100 ms to 1 s range is discussed. Departures of the behavior of the accumulator from that expected of such an instrument are presented. The utility of these effects in diagnosing accumulator performance is described. © *2006 American Institute of Physics.*
[DOI: 10.1063/1.2206561]

## I. INTRODUCTION

The production and manipulation of laboratory-based low energy positron beams is now routine, and there have been widespread applications, particularly in atomic and condensed matter physics (see, e.g., Refs. 1–3 for reviews). Over the years many of these applications have utilized time-tagged beams, in which the time of flight of individual positrons has been monitored and used in energy analysis and/or to provide angular discrimination in scattering experiments. Devices capable of providing narrow time-width pulses containing a few positrons have also been developed and applied.[4,5] More recently, the potential to exploit positron plasmas accumulated in vacuum has begun to be realized. There have been notable achievements in atomic scattering and annihilation[6–8] and in facilitating the creation of cold antihydrogen.[9–11] This emerging and many-faceted area of science has recently been reviewed.[12] A review of a number of positron accumulation schemes in the context of antihydrogen physics is also available.[13]

This article describes a compact positron accumulator. It is based upon the buffer gas cooling method, pioneered by Surko and co-workers,[14,15] in which molecular nitrogen gas is used to capture and cool positrons from a low energy beam. The accumulator is a variety of the well-known Penning-Malmberg trap[16] in which axial confinement is provided by the electrical potential formed by applying voltages to an array of cylindrical electrodes, while radial confinement is assured by the presence of a uniform axial magnetic field.

The most established operational buffer gas-cooled positron accumulators are three-stage devices. In these, the first, high pressure (around $10^{-3}$ mbar) stage is used to capture a fraction of the incident positrons via an inelastic collision with the gas molecule. Further such collisions on the microsecond to millisecond time scale transfer the positrons to the second and, finally, the third stage, wherein they are accumulated and thermalized (typically to the gas temperature, 300 K). Each of the consecutive stages has progressively increasing electrode diameters, such that the gas pressure lowers from stage to stage. (Note that the gas is admitted to the electrodes at the center of the first stage.) Typical pressures in the third stage are around $10^{-6}$ mbar, resulting in positron annihilation lifetimes of around 100 s. The number of trapped positrons saturates when the accumulation rate and the annihilation rate are equal. The former depends upon the trapping efficiency and the incident positron flux. Using solid neon moderators to produce the slow positron beam,[17–19] $10^8$ trapped positrons can be achieved routinely.[19,20] More positrons can be accumulated in higher vacuum. This can be achieved by a further (fourth) storage stage to which the positrons can be transferred and then stacked. Such a scheme is being implemented by the UCSD group[21] and has been achieved by the ATHENA antihydrogen collaboration, whose current record[22] for positron numbers stands at around $10^9$.

It has, however, been pointed out that transfer to a high vacuum stage with storage times of the order $10^3$ s can be achieved by utilizing a two-stage trap, with a concomitant simplification (and cost reduction) of the apparatus.[23] Further, such an advance would produce a standalone two-stage trap for applications, for instance, in which more modest positron fluxes were required. In parallel with this initiative (see Ref. 24) we have been developing a two-stage trap, which we describe herein, for operation as a pulsed source of positrons and positronium atoms, in the 1–100 Hz range, with a timing resolution of the order 10–20 ns. In particular, we wish to interface the output of this device to that of a 10 Hz, 10 ns wide pulsed laser system designed for spectroscopic investigations of positronium.

In this article we will describe the design, construction, and operation of our two-stage trap. This will be mainly covered in the following two sections, the second of which will contain detailed results of our investigations into the performance of the accumulator.

## II. DESIGN AND APPARATUS DETAILS

The global design parameters of the instrument were governed by its physics applications. The burst of positrons was to be used to create a timed source of positronium atoms following their interaction with a target formed from a suitable material surface. Our aim was to produce a flux of up to $10^5$ positronium atoms in a sharp burst (10–20 ns wide) every 100 ms. This would allow interaction of the positronium

 

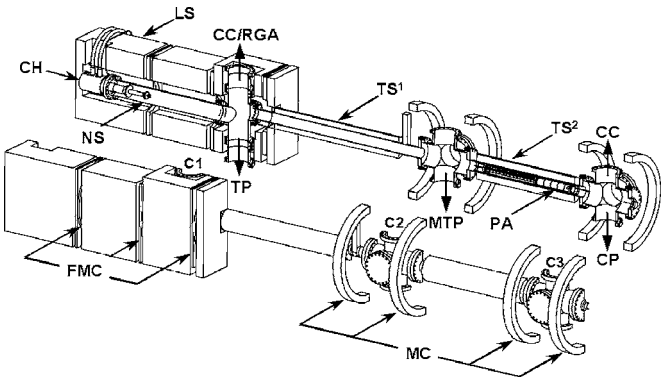


FIG. 1. Cutaway diagram of the positron beam line showing the positions of the source, positron accumulator, and various magnetic steering fields. From left to right in the diagram the vacuum crosses are numbered C1, C2, and C3. The six-way crosses C2 and C3 are pumped by a magnetically levitated turbomolecular MTP and cryopump CP, which are jointly backed, by an 11 $m^3/h$ scroll pump. The four-way cross C1 is pumped using a turbomolecular pump TP backed by a second 11 $m^3/h$ scroll pump. Key: CH, cold head; NS, $^{22}Na$ source; LS, lead shielding; PA, positron accumulator; CC, cold cathode pressure gauge; RGA, residual gas analyzer; FMC, flat magnetic coils; $TS^1$, transport solenoid; $TS^2$, trap solenoid; MC, magnetic coil.

atoms with photons from laser beams which cross the region directly in front of the positron target. Furthermore, the timed positron pulse is to be transported into a high magnetic field (5 T) in an effort to study the production of Rydberg magnetized positronium, as recently observed.[25] The modest timing and storage time requirements meant that a two-stage trap could be utilized without further pulse compression.[12,23] The desired positronium yield mandated the use of a solid neon moderator, with a strong radioactive source.

Detailed drawings of the apparatus showing the main components of the entire instrument and the electrodes of the accumulator are given in Figs. 1 and 2. Our source end configuration is based upon that developed for the ATHENA antihydrogen experiment.[20,26] Positrons are derived from a

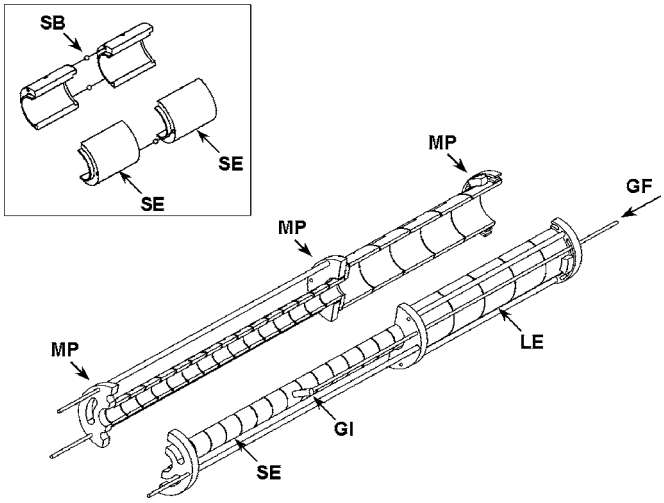


FIG. 2. Cutaway diagram of the positron accumulator consisting of 15 small electrodes of internal diameter of 16 mm and five large electrodes of internal diameter of 41 mm, insulated from each other by three 2 mm diameter sapphire balls (see insert). The mounting plates were precision machined to fit snugly inside the 66 mm internal diameter vacuum tube. Key: GI, gas inlet; GF, gas flow; SB, sapphire balls; [MP], mounting plates; LE, large electrodes; SE, small electrodes.

1 GBq (27 mCi) $^{22}Na$ radioactive source that, together with a cone-shaped extension, is mounted directly on the cold finger of a closed cycle helium refrigerator. The base temperature of the cold head is around 7 K. The deposition of neon onto the source and cone, typically at a chamber pressure of $5\times10^{-4}$ mbar, is done at this temperature. During deposition, which typically lasts around 60 min, the slow positron counts are monitored continuously. The beam is guided away from the source region using axial magnetic fields provided by a series of coils, and a 500 G transport solenoid ($TS^1$ in Fig. 1), and annihilates on a vacuum valve about 1.5 m downstream. The resulting gamma-ray flux is monitored using a CsI-photodiode detector assembly. After optimization, beam strengths of around $(3-4)\times10^6$ positrons/s can be obtained, with an ~3 eV full width at half maximum (FWHM) energy resolution. Further details of some of our experimentation with solid neon moderators can be found elsewhere.[24] The beam diameter was measured by lowering a metal plate progressively through the beam and measuring the ensuing annihilation radiation. The differential of these measurements gave the beam profile, which could be fitted by a Gaussian with a diameter of around 12 mm full width.

In order to keep the solenoid to be used in the accumulation region as compact as possible, the largest electrodes that could be used had to fit inside a tube limited by flange sizes to an internal diameter of 66 mm. (The trap solenoid, $TS^2$ in Fig. 1, was wound onto a water-cooled former of 140 mm diameter and comprised three layers of around 170 turns each. When powered at 31 V and 44 A it produced a magnetic field on axis of around 400 G.) The two-stage electrode structure of the trap is shown in Fig. 2 and illustrated schematically in Fig. 3(a). The first stage is comprised of 15 gold-plated electrodes of internal diameter of 16 mm and length of 24 mm. They are biased electrically with respect to the solid neon moderator voltage and have a small potential difference across them [as shown in Fig. 3(b)] of around 2 V. (This increased the number of trapped positrons by approximately 25% over the best achieved with equipotential electrodes in stage 1.) The nitrogen buffer gas is piped into the accumulator through a small hole (marked GI in Fig. 2) bored in the eighth electrode of this stage. The second stage consists of five electrodes, also gold plated, of internal diameter of 41 mm and length of 49 mm. Thus, the entire trap is around 650 mm in length and is pumped on one end by an APD8 cryopump (800 l $s^{-1}$ pumping speed for $N_2$), and on the other by a Leybold 340M magnetically levitated turbomolecular pump (400 l $s^{-1}$ pumping speed for $N_2$). The two sections of the trap are held together by rods attached to three mounting plates, one at either end and one between the two stages. The trap is assembled electrode by electrode, using 2 mm diameter sapphire balls as interelectrode spacers. Each electrode can be biased independently.

The electrical potential (on axis) in the accumulation region is shown in Fig. 3(b). The potential well and reflecting wall were effected in stage 2 of the trap. The gas pressure in stage one was set to be around $10^{-3}$ mbar, falling (from calculation) to below $10^{-4}$ mbar in stage 2. The gas pressure was measured in the vacuum chamber at the exit of the sec-

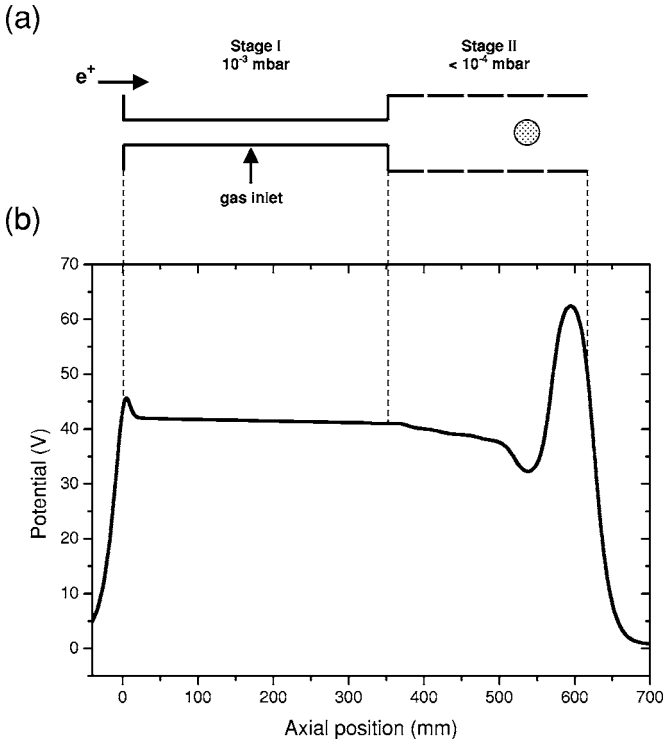


FIG. 3. (a) Schematic illustration of the electrode structure of the accumulator. (b) The electrical potential along the axis of the trap.

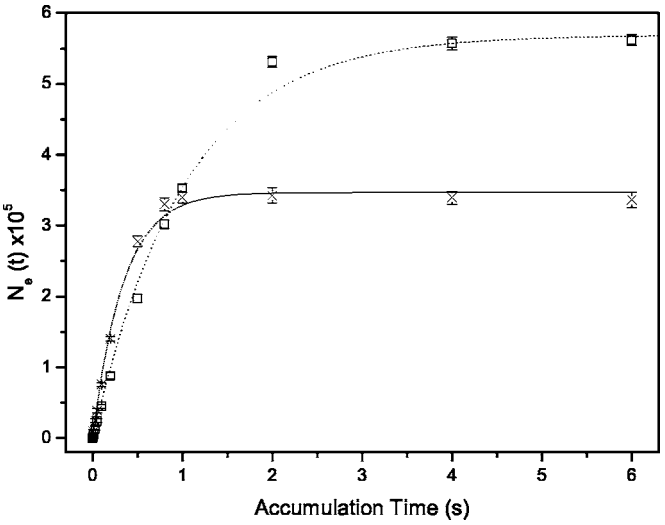


FIG. 4. Accumulation curves at pressures of $6\times10^{-6}$ (squares) and $2\times10^{-5}$ (crosses) mbar. The lines are fits to Eq. (1).

ond stage of the accumulator using a cold cathode gauge and also on the gas input line using a capacitance manometer. The latter was used for pressure stabilization effected via a LABVIEW™ program and a piezoelectric leak valve. The measured chamber pressures were varied in the range of $5\times10^{-7}$ to $3.5\times10^{-5}$ mbar dependent upon the experiment being undertaken. The base pressure was around $10^{-9}$ mbar.

The positrons could be accumulated for the desired period and then ejected onto an annihilation target by lowering the reflecting wall to ground. The sharp burst of gamma rays emitted as a result of the pulsed ejection was integrated by a CsI-photodiode detector located in close proximity to the target. This detector was read out via an oscilloscope. To relate the signal from this detector to the absolute number of stored positrons required a calibration to be undertaken. The pulsed output of the detector was normalized following the procedure developed by ATHENA using calibrated gamma-ray sources[26] for reference. Following this we estimate that the absolute positron numbers are accurate to ±10%. The dc beam (i.e., without the accumulator in operation) was monitored using the CsI detector, and also a calibrated HPGe detector. In this instance the CsI was calibrated against an in-beam channeltron detector using standard coincidence techniques. Using this combination of normalizations, parameters relating to the efficiency of the accumulator could be derived (see Sec. III).

A channeltron detector was used to derive the timing characteristics of the pulsed output of the accumulator. In this case the accumulator output (reflecting) electrode voltage was driven by a fast amplifier with a 35 ns fall time from 100 V to ground. This meant that the voltage across the space charge of the accumulated positron cloud was lowered to allow escape in a 0.4 ns time window. In this case, before ejection, the potential well was squeezed for 1 ms by raising the bias applied to all electrodes except the penultimate electrode in stage 2 by 60 V. The latter was raised by 50 V.

Control of the entire system was achieved using specially developed LABVIEW™ programs. This included control of all of the electrode voltages, and changes to them for trap-and-dump cycles which did not require fast timing, the gas pressure system, and various triggers for the detectors.

## III. OPERATION AND RESULTS

The accumulator was used to trap positrons with the on-axis potential shown in Fig. 3(b). The physical basis for the operation of the device was summarized in Sec. I and more details can be found elsewhere.[15] Once the desired accumulation time had been reached the positron beam was prevented from entering the trap, and the confining well was squeezed, whence the confining potential was lowered and the positron bunch was ejected and directed along the beam line to an annihilation target. The resulting gamma-ray signal was used to derive information on the number of positrons trapped, their lifetime, and the time width of the positron pulse. This so-called "trap-and-dump" cycle could be varied at will, depending upon the application, though in practice the minimum accumulation time we used was 20 ms.

Figure 4 shows examples of accumulation curves taken at pressures (see Sec. II) of $6\times10^{-6}$ and $2\times10^{-5}$ mbar. In these cases the positrons were accumulated for varying times and the number of positrons trapped, $N_e(t)$, recorded. The accumulation curves take the form

$$N_e(t) = A(1 - e^{-t/\tau}), \tag{1}$$

where $\tau$ is the lifetime of the positrons in the second stage of the accumulator and $A=R\tau$, where $R$ is the positron accumulation rate. The latter is the product of the beam intensity $I_o$ and the trapping efficiency (per positron) $\varepsilon$. At short times the gradient of $N_e(t)$ allows $R$ to be extracted. With a beam intensity of $3.4\times10^6 e^+\ s^{-1}$ (see below) $R$ is around 29%. It is clear from (1) that saturation occurs when

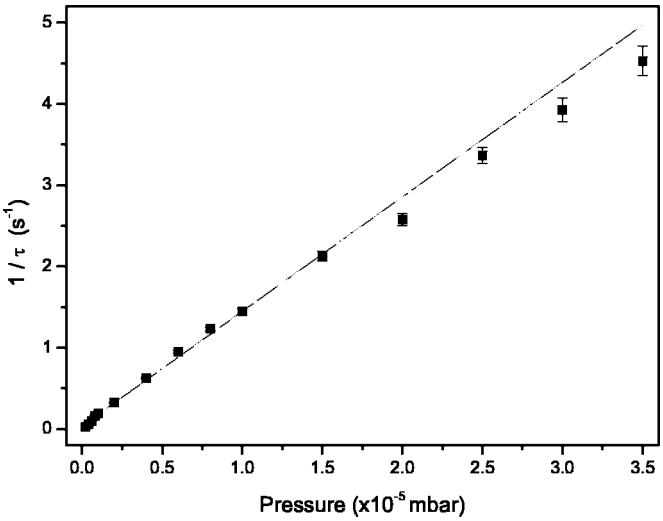


FIG. 5. Plot of the inverse of the measured positron lifetime $(1/\tau)$ vs the gas pressure. The plotted line is the result of a weighted least squares fit.

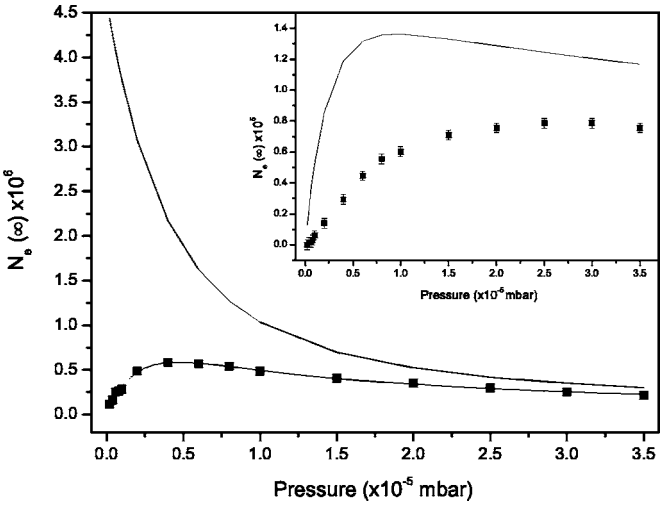


FIG. 6. Measured saturation intensity $N_e(\infty)$ at various gas pressures. The data are fit to Eq. (5). The curve shows the behavior expected from an ideal accumulator [Eq. (4)]. Inset: a comparison of the ideal and the real behavior of the accumulator for 100 ms operation.

$$N_e(\infty) = A. \tag{2}$$

Fits of (1) to the accumulation curves are shown in Fig. 4, from which values for $A$ and $\tau$ can be extracted. Accumulation experiments were repeated at several different pressures. The results for positron lifetimes at the various measured pressures $P$ (which are dominated by that of the $N_2$ buffer gas) are shown in Fig. 5. At the low pressures used in these experiments the positron annihilation rate is strictly proportional to gas density (and hence $P$), such that a straight line should be obtained by plotting $1/\tau$ vs $P$ (Fig. 5). (The cause of the deviation from the fitted line at the higher pressures is not known.) In principle there could be more than one contribution to the positron annihilation rate; for example, annihilation on the nitrogen buffer gas might also be accompanied by annihilation on the rest of the gas in the vacuum chamber. Despite the fact that the base pressure in the vacuum chamber is around $10^{-9}$ mbar, the latter is potentially serious, even for very small quantities of certain hydrocarbons (see, e.g., Ref. 27). If this were the case the positron lifetime could be found from

$$1/\tau = BP + C, \tag{3}$$

where $B$ is a constant at fixed temperature and is related to the $Z_{\text{eff}}$ of $N_2$, the effective number of electrons in the molecule available to the positron for annihilation.[27,28] It also includes the ratio of the measured pressure to that pertaining in the second stage of the trap where the positrons are accumulated. $C$ is the constant due to the residual background gas. Thus, it will be immediately apparent, upon inspection of the zero $P$ intercept of a $1/\tau$ vs $P$ plot, whether there is any influence from annihilation on the residual background gas. It is clear from Fig. 5 that this is negligible for our accumulator.

Further information on the performance of the accumulator can be gleaned by inspecting the pressure dependence of $N_e(\infty)$. Ideally, this quantity should behave, from above, according to

$$N_e(\infty) = A = I_o \varepsilon \tau = f I_o (1 - e^{-DP})/BP, \tag{4}$$

when $C=0$. Here $f$ is a branching ratio determined by the ratio of the cross section for the electronic excitation of the molecule in a positron-$N_2$ collision (which promotes trapping) to that for other processes (positronium formation being dominant) which remove positrons from the beam. The constant $D$ is related to the total scattering cross section for positron-$N_2$ collisions. At high pressures this function behaves as $1/P$, while it tends to a constant value $(fI_oD/B)$ as $P \to 0$. Figure 6 shows the behavior of $N_e(\infty)$ vs $P$ for our accumulator. While the $1/P$ form is found at high $P$, the expected trend at low pressures is not observed. Indeed, a good fit to a linear form in $P$ can be obtained in this region.

Possible reasons have been explored for this behavior, as we now note. We observe that (4) for the ideal accumulator contains a hidden assumption. The form of (4) is governed by two contributions: the rate of capture into the first stage multiplied by the lifetime of the positrons in the second stage. The implicit assumption is that positrons are transferred from stage 1 to stage 2 two with unit efficiency. If, instead, we postulate that there is a pressure-independent loss at this junction parametrized by a further constant $F$, then an extra branching ratio factor must be introduced. This has the generic form $EP/(EP+F)$, where $E$ is a constant and the term $EP$ represents the probability of capture into stage 2. This has the effect of modifying (4) to become

$$N_e(\infty) = f I_o E (1 - e^{-DP})/B(EP + F). \tag{5}$$

This expression retains the $1/P$ dependence at high $P$, but at low $P$ when $F \gg EP$ and $DP \ll 1$, we find $N_e(\infty) \propto P$, as observed. A similar form could also be recovered if $C \neq 0$ and (3) was used for the positron lifetime, rather than $BP$. However, this can be ruled out by inspection of Fig. 5.

The presence of a pressure-independent loss between the two stages of the accumulator may arise due to the effects of a mechanical misalignment of the electrodes of the trap and/or a field misalignment. Both of these could cause transport of the particles to the wall, particularly as they typically

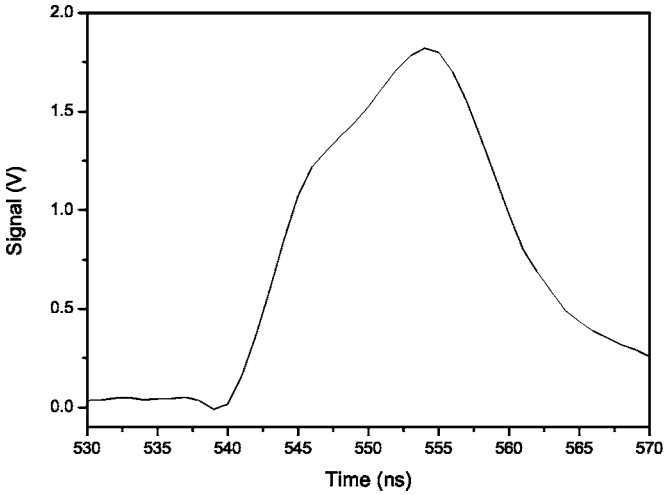


FIG. 7. Timing resolution of the accumulator output as measured using the channeltron detector.

have to traverse the narrow bore electrodes of stage 1 several times before capture into stage 2 occurs. Such trap imperfections are also known to cause plasma instabilities and particle loss on longer time scales.[29–31] To date we have been unable to locate the source of the misalignment in the system; however, the methodology is sound and represents a useful trap diagnostic.

From the fitted parameters derived from Figs. 5 and 6 ($fI_o$, $B$, $D$, and $F/E$) we have been able to plot the curve [Eq. (4)] for the ideal accumulator. This is also shown in Fig. 6. Although an ideal accumulator has the potential to store nearly an order of magnitude more positrons than our current maximum of $6\times10^5$, for our purposes the deficit is much smaller. The 10 Hz repetition rate demands accumulation at the high pressure end of our range. The inset in Fig. 6 shows the real and ideal curves for 0.1 s accumulation time calculated using the fitted parameters mentioned above. Note that we are able to isolate $fI_o$ from this analysis to be around $1.5\times10^6$. From Sec. II we note that $I_o=3.4\times10^6$, such that $f=0.44\pm0.04$. (The uncertainty is dominated by that on the absolute positron number scale.) Such a value for $f$ is not unreasonable given the resonancelike behavior in the near-threshold electronic excitation cross sections for positrons[8] on $N_2$.

The timing characteristics of the accumulator output are also important for our application. The timing resolution was measured, as described in Sec. II, by monitoring the output of an in-beam channeltron detector. An example of the timing spectrum taken directly from the oscilloscope is shown in Fig. 7 and reveals that the resolution is around 15 ns FWHM. This is measured at a target 0.3 m downstream from the exit electrode of the accumulator. This resolution is adequate for our purposes such that we have made no attempts to optimize this output. We anticipate that improvements could be made by using a higher voltage pulser to drive the accumulator output, or as demonstrated elsewhere by using an ancillary electrode to achieve timed potential bunching.[12,23]

## ACKNOWLEDGMENTS

The authors are grateful to R. G. Greaves and C. M. Surko for useful discussions and to the technical support staff at UWS for their assistance. The authors thank the EPSRC for the financial support of this work under award No. GR/R/81541/01.

[1] M. Charlton and J. W. Humberston, *Positron Physics* (Cambridge University Press, Cambridge, 2001), p. 454.
[2] *Positron Beams and Their Applications*, edited by P G. Coleman (World Scientific, Singapore, 2000), p. 322.
[3] *New Directions in Antimatter Chemistry and Physics*, edited by C. M. Surko and F. A. Gianturco (Kluwer Academic, Dordrecht, 2001), p. 511.
[4] A. P. Mills, Jr., Appl. Phys. **22**, 273 (1980); W. S. Crane and A. P. Mills, Jr., Rev. Sci. Instrum. **56**, 1723 (1985).
[5] J. P. Merrison, M. Charlton, P. Aggerholm, H. Knudsen, D. P. van der Werf, J. Clarke, and M. R. Poulsen, Rev. Sci. Instrum. **74**, 3284 (2003).
[6] S. J. Gilbert, L. D. Barnes, J. P. Sullivan, and C. M. Surko, Phys. Rev. Lett. **88**, 043201 (2002).
[7] L. D. Barnes, S. J. Gilbert, and C. M. Surko, Phys. Rev. A **67**, 032706 (2003).
[8] J. P. Sullivan, J. P. Marler, S. J. Gilbert, S. J. Buckman, and C. M. Surko, Phys. Rev. Lett. **87**, 073201 (2001).
[9] M. Amoretti *et al.*, Nature (London) **419**, 456 (2002).
[10] M. Amoretti *et al.*, Phys. Lett. B **578**, 23 (2004).
[11] M. Amoretti *et al.*, Phys. Lett. B **583**, 59 (2004).
[12] C. M. Surko and R. G. Greaves, Phys. Plasmas **11**, 2333 (2004).
[13] M. Holzscheiter, M. Charlton, and M. M. Nieto, Phys. Rep. **402**, 1 (2004).
[14] C. M. Surko, M. Leventhal, and A. Passner, Phys. Rev. Lett. **62**, 901 (1989).
[15] T. J. Murphy and C. M. Surko, Phys. Rev. A **46**, 5696 (1992).
[16] J. S. deGrassie and J. H. Malmberg, Phys. Rev. Lett. **39**, 1077 (1977).
[17] A. P. Mills, Jr. and E. M. Gullikson, Appl. Phys. Lett. **49**, 1121 (1986).
[18] R. Khatri, M. Charlton, P. Sferlazzo, K. G. Lynn, A. P. Mills, Jr., and L. O. Roellig, Appl. Phys. Lett. **57**, 2374 (1990).
[19] R. G. Greaves and C. M. Surko, Can. J. Phys. **74**, 445 (1996).
[20] D. P. van der Werf, L. V. Jørgensen, T. L. Watson, M. Charlton, M. J. T. Collier, M. Doser, and R. Funakoshi, Appl. Surf. Sci. **194**, 312 (2002).
[21] J. R. Danielson, P. Schmidt, J. P. Sullivan, and C. M. Surko, AIP Conf. Proc. **692**, 149 (2003).
[22] L. V. Jørgensen *et al.*, Phys. Rev. Lett. **95**, 025002 (2005).
[23] R. G. Greaves and J. Moxom, AIP Conf. Proc. **692**, 140 (2003).
[24] J. Clarke, D. P. van der Werf, M. Charlton, D. Beddows, B. Griffiths, and H. H. Telle, AIP Conf. Proc. **692**, 178 (2003).
[25] J. Estrada, T. Roach, J. N. Tan, P. Yelsey, and G. Gabrielse, Phys. Rev. Lett. **84**, 859 (2000).
[26] M. Amoretti *et al.*, Nucl. Instrum. Methods Phys. Res. A **518**, 679 (2004).
[27] K. Iwata, R. G. Greaves, T. J. Murphy, M. D. Tinkle, and C. M. Surko, Phys. Rev. A **51**, 473 (1995).
[28] G. R. Heyland, M. Charlton, T. C. Griffith, and G. L. Wright, Can. J. Phys. **60**, 503 (1982).
[29] J. H. Malmberg and C. F. Driscoll, Phys. Rev. Lett. **44**, 654 (1980).
[30] J. Notte and J. Fajans, Phys. Plasmas **1**, 1123 (1994).
[31] M. C. Fujiwara *et al.*, Phys. Rev. Lett. **92**, 065005 (2004).